jet INTL JOURNAL OF ELECTRONICS AND TELECOMMUNICATIONS, 2023, VOL. 69, NO. 1, PP. 61-67
Manuscript received May 29, 2022; revised February, 2023. DOI: 10.24425/ijet.2023.144332

Passive Mixer-based UWB Receiver with Low Loss, High Linearity and Noise-cancelling for Medical Applications

Thaar A. Kareem, and Hatem Trabelsi

***Abstract*—A double balanced passive mixer-based receiver operating in the 3-5 GHz UWB for medical applications is described in this paper. The receiver front-end circuit is composed of an inductorless low noise amplifier (LNA) followed by a fully differential voltage-driven double-balanced passive mixer. A duty cycle of 25% was chosen to eliminate overlap between LO signals, thereby improving receiver linearity. The LNA realizes a gain of 25.3 dB and a noise figure of 2.9 dB. The proposed receiver achieves an IIP3 of 3.14 dBm, an IIP2 of 17.5 dBm and an input return loss (S11) below -12.5dB. Designed in 0.18µm CMOS technology, the proposed mixer consumes 0.72pW from a 1.8V power supply. The designed receiver demonstrated a good ports isolation performance with LO_IF isolation of 60dB and RF_IF isolation of 78dB.**

***Keywords*—WBAN; UWB receiver; LNA; passive mixer; linearity; ports isolation**

I. Introduction

THE development of ultra-low power consumption wireless communication ICs for medical applications is a major challenge [1]. These ICs should meet the following characteristics: small size, low complexity, low noise and low power consumption [2,3].

The deployment of an ultra-wide band (UWB) communication system in medical applications is highly desirable [4] because of its potential advantages, such as low probability of interception, promotion of the coexistence with existing wireless communication systems, increased data rates [5], decreased power dissipation and enhanced security of medical data, due to the -41.3 dBm/MHz power spectral density emission limit. [6].

Because of the wide frequency range of the UWB signal, it may penetrate biological materials including skin, fat, and other organic tissues, and the reflection from interior organs allows for vital sign monitoring [7].

The UWB wireless body area network (UWB-WBAN) is well-known for providing a reliable, low-power, optimised wireless connection between worn transceivers for physiological signal monitoring [8,9]. With the improvement of the CMOS technology, the receiver's front end can now be optimised for linearity, noise figure (NF), low power and chip area [10,11].

Currently, UWB systems are essentially established on two schemes, namely, orthogonal frequency division multiplexing (OFDM) and impulse radio (IR). On the one hand, although OFDM-UWB can provide a reliable broadband solution, it does so at the expense of circuit complexity and energy consumption due to the need for intensive digital signal processing [11]. The IR-UWB system, on the other hand, has been shown to be accommodated at low power consumption and provides simple transceiver topologies that can be readily integrated on a minimal chip area due to its intrinsically cyclical nature [12,13].

The objective of this research work is to design an innovative solution for the receiver part of a wireless sensor node device that maximizes the autonomy in a WBAN. The receiver uses a 25% duty cycle double balanced passive mixer with NMOS switches.

This paper is organised as follows. Section II presents the proposed receiver architecture. The low noise amplifier (LNA) circuit design and simulation are presented in Section III. Section IV discusses the receiver design with a differential double-balanced down-conversion passive mixer. This section presents and discusses time domain as well as frequency domain simulation results. Finally, Section V concludes this paper.

II. RECEIVER ARCHITECTURE

The transceiver architecture is shown in Fig. 1. Hardware minimisation can be achieved by using a direct conversion architecture that eliminates the image-reject filter and other IF components, enabling a monolithic transceiver [14,15].

The transmitting chain consists of an UWB pulse generator, a chirp FSK modulator followed by a power amplifier and an antenna. Depending on the transmitter binary information input, the chirp FSK modulator generates a dual-band FSK modulated signal by switching between two sub band signals. The antenna emits the modulated signal once it has been amplified by the power amplifier.

The received signal is first amplified with a LNA. The UWB RF differential LNA signal drives the input of a differential double-balanced down-conversion passive mixer. Four rectangular LO signals with a 25% duty-cycle LO wave set to 4 GHz drive the mixer switches. The differential double-balanced down-conversion passive mixer is connected to the LNA through AC coupling capacitor to isolate the LNA and mixer DC voltages and block the LNA second-order intermodulation products signals. The mixer operates in voltage mode and is loaded with capacitors C_{IF} and a voltage amplifier. Resistors R_B are used to set the mixer bias.

A low pass filter (LPF) is often used to filter the voltage amplifier's output signal .The latter passes only the selected

Authors are with Systems Integration & Emerging Energies Laboratory, Electrical Engineering Department, National Engineers School of Sfax, University of Sfax, Sfax, Tunisia (e-mail: thaar_kareem@uomisan.edu.iq, hatem.trabelsi@enis.tn).

down-converted channel signal and suppresses the other channel. Finally, the chirp FSK demodulator will retrieve the digital transmitted data [5]. Given that the I and Q channels are active at the same time, the 50% duty cycle mixer suffers from IQ crosstalk and its effects on linearity and noise. Then, the Q channel loads the I channel, and vice versa. This phenomenon does not occur in the case of the 25%-duty-cycle mixer, where only one channel is active at any given time.

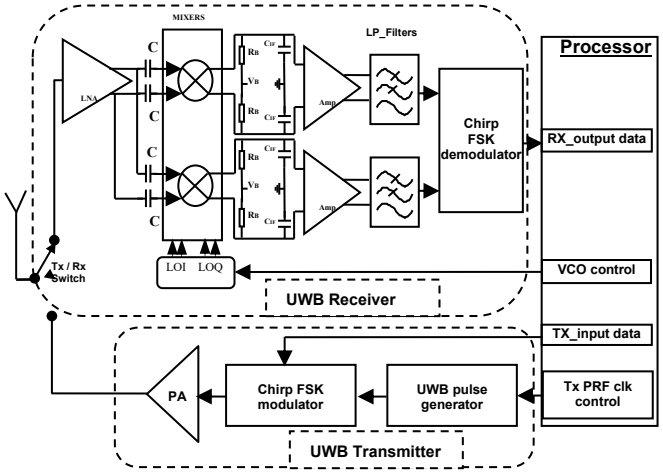

Fig. 1. Front-end topology of the UWB transceiver

The IQ crosstalk in a 25%-duty-cycle mixer is much lower than in a 50%-duty-cycle mixer. The CMOS passive mixer has good linearity and no DC power, except for its clock generation circuit and is less dependent on process variations and has a smaller die area and a better LO-RF feed through performance than an active mixer. Moreover, the LNA, LPF and down-conversion passive mixer is designed differentially to reduce the second-order nonlinearity and cancels common-mode noise.

III. LNA CIRCUIT DESIGN

A. LNA circuit

Designing a wideband LNA is one of the major challenges in the design of an UWB communication system [16]. As the first active element in the receive chain, the LNA must achieve sufficient gain while incurring a small additional noise to minimize the overall receiver noise figure (NF). Furthermore, the LNA must provide good linearity while consuming low power [16,17]. The differential LNA offers several advantages, such as the rejection of the noise travelling in the substrate, the supply noise and attenuates the common mode signal.

Proposals for wideband LNAs with cancelations of noise and distortion have been recently reported in[18]. Thus, a balun is needed at some point in the receiving chain to convert the single-ended RF signal into a differential signal [19]. Broadband passive baluns usually have large losses that greatly degrade the total NF of the receiver.

The proposed circuit of the differential LNA is shown in Fig. 2. The circuit features a differential output and a single-ended input. The single-ended input facilitates the connection to the RF antenna. Fig. 2 illustrates a wideband LNA scheme that employs the common gate (CG) stage (M1,M3) as an input while using a common source (CS) stage (M2,M4) for the differential output and the noise cancellation [20]. Therefore, the combination of balun and LNA leads to noise cancellation that is achieved by the identical gain of the CG and CS stages. A clearly defined impedance for wideband matching at the RF input port may be readily achieved by setting the transconductance of M1 to 50Ω. The CG stage has greater linearity than the CS stage [21]. The PMOS M3 and M4 transistors configured as load enable the maximum gain and minimize the NF. The supply, CG bias and PMOS bias voltages are denoted by V_{dd}, V_{bias1} and V_{bias2}, respectively.

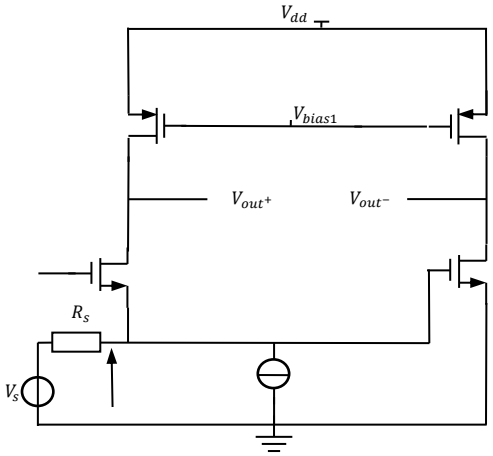

Fig. 2. Proposed Balun LNA circuit

G_{cg} denotes the voltage gain of the CG stage and G_{cs} is the voltage gain of the CS stage. They are given by the following equations:

$$G_{cg} = \frac{V_{out}^{+}}{V_{in}} = \frac{r_{03}(1+g_{m1}r_{01})}{r_{03}+r_{01}} \quad (1)$$

$$G_{cs} = \frac{V_{out}^{-}}{V_{in}} = -g_{m2}\frac{r_{02}r_{04}}{r_{02}+r_{04}} \quad (2)$$

where r_{01}, r_{02}, r_{03} and r_{04} are the output resistances of transistors M1, M2, M3 and M4 respectively. g_{m1} and g_{m2} are the transistor's M1 and M2 transconductances, respectively.

The gain for the LNA is equal to:

$$G_{LNA} = \frac{V_{out}^{+} - V_{out}^{-}}{V_{in}} \quad (3)$$

To have a differential output circuit and cancel the output noise, the magnitude of the two gains should be equal. This objective can be achieved if we make $r_{o3} = r_{o4} = r_{oPmos}$, $r_{o1} = r_{o2} = r_{oNmos}$, $(g_{m1} + g_{mb1})r_{o1} \gg 1$, $g_{m1} = g_{m2}$ and ignore the transistor body effect. The LNA gain will then be expressed as follows (4):

$$G_{LNA} = \frac{(V_{out}^{+} - V_{out}^{-})}{V_{in}} = G_{CG} - G_{CS} = 2g_{m1}\frac{r_{oNmos}\, r_{oPmos}}{r_{oNmos}+r_{oPmos}} \quad (4)$$

Indeed, to attain the best performance, a suitable scaling of the CS stage is required not only for a low NF but also for low distortion. The nonlinearity of transconductance g_{m2} and output conductance g_{ds2} is the principal cause of this distortion in addition to the dependence of g_{m2} on the drain source bias voltage [21]. Moreover, the best LNA linearity performance is obtained if the CS stage has a good linearity.

The input impedance of the LNA is very significant for the overall receiver performance. The impedance of the LNA input is the result of the CG input impedance (Z_{inCG}) in parallel with the CS input impedance (Z_{inCS}). However, the design was made considering an extremely high Z_{inCS}. Therefore, the LNA input impedance will be:

$$Z_{inLNA} = Z_{inCG} \approx \frac{1}{g_{m1}} \quad (4)$$

Thus, the correct size of the M1, M2, M3 and M4 transistors is determined to provide the best input impedance matching, Rs = 50Ω and an equal gain for the CG and CS stages.

B. LNA simulation results

The results of the analysis and simulation of the proposed wideband LNA were evaluated in terms of gain, NF and linearity. Simulation was conducted with the Advanced Design System (ADS) tool and the TSMC RF 0.18 µm CMOS design kit process.

1) Gain, S11 and NF

The input return loss S_{11} plot in Fig. 3 shows that S_{11} is less than -10 dB for the frequency range of 3–5 GHz, indicating that the designed LNA is considered input matched in this frequency band. Fig. 4 shows that the LNA gain ranges from 22 dB to 25.3 dB for the 3 GHz to 5 GHz frequency, indicating a good gain performance. As shown in Fig. 5, the NF varies from 2.9 dB to 3.2 dB for the 3 GHz to 5 GHz frequency.

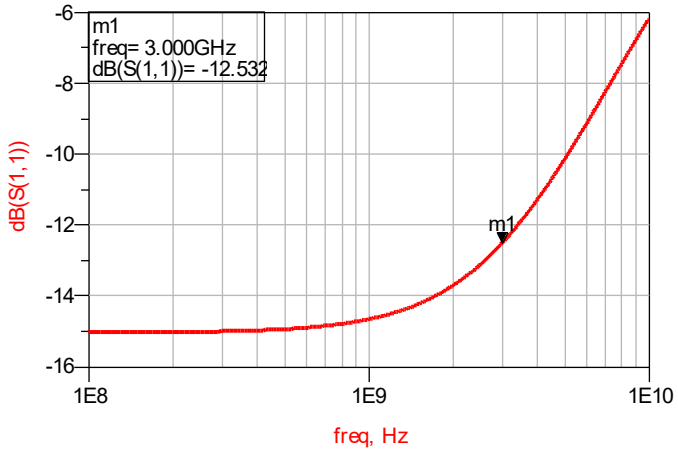

Fig. 3. S11 in dB of the LNA

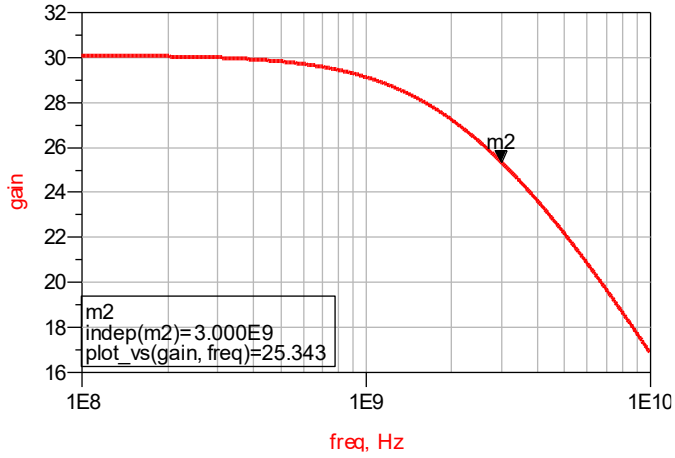

Fig. 4. Gain in dB of the LNA

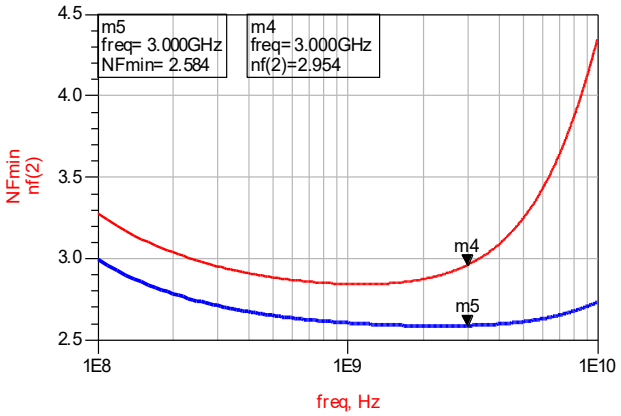

Fig. 5. NF of the LNA

2) P-1dB, IIP3 and IIP2

Harmonic balance simulations were conducted to evaluate the LNA linearity performance. The distortion performance was analyzed for second and third-order intermodulation intercept inputs IIP2 and IIP3 and is depicted in Fig. 6 and Fig. 7. An IIP3 of 1.5 dBm and an IIP2 of -3.9 dBm were achieved. As shown in Fig. 8, the LNA 1 dB compression point (P_{-1dB}) equals to -14 dBm. Given that the UWB receiver receives a maximum power of -41.3 dBm/MHz, the values found by simulation show that the LNA has an excellent linearity performance. The proposed wideband LNA consumes 7.6 mW at a supply voltage of 1.8 V.

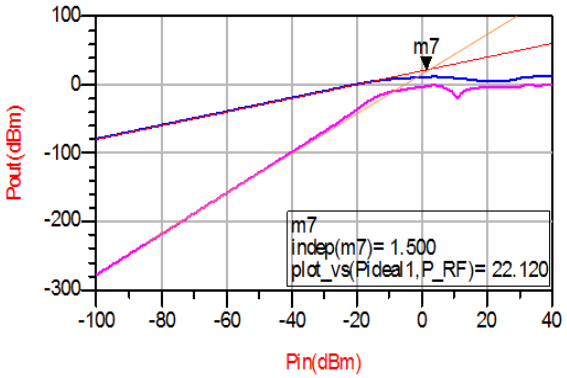

Fig. 6. IIP3 of the LNA

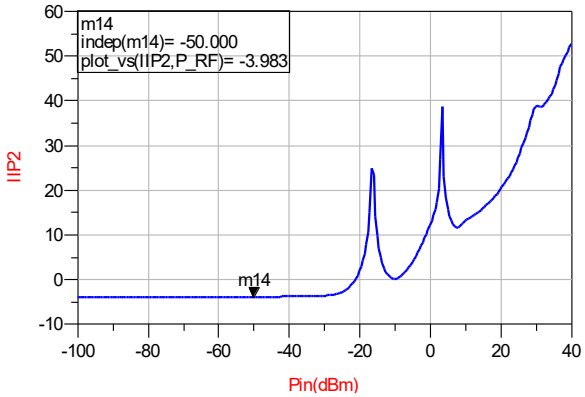

Fig. 7. IIP2 of the LNA

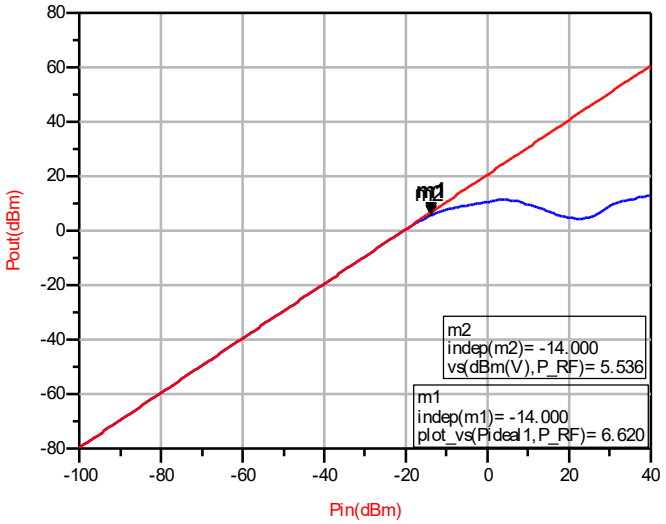

Fig. 8. P_{-1dB}(in dBm) of the LNA

IV. PROPOSED PASSIVE MIXER-BASED UWB RECEIVER

A. *Passive mixer-based UWB receiver circuit*

Compared to an active mixer, the main advantages of a passive mixer include low power consumption, low 1/f noise and good linearity. The LO feed-through in the single-balanced passive mixer is generated by DC current in the RF input[14,22]. As a result, we selected a double-balanced passive mixer with a fully differential architecture to avoid LO feed-through.

The passive mixer-based UWB receiver circuit is depicted in Fig. 9. First, the LNA amplifies the UWB RF signal coming from antenna. Then the differential RF signal VLNAout is down-converted by the double-balanced passive mixer and appears through the baseband load ($C_{IF} \parallel R_B$). To prevent the DC bias and the second-order intermodulation components produced inside the LNA, capacitors (C) are added in each mixer input.

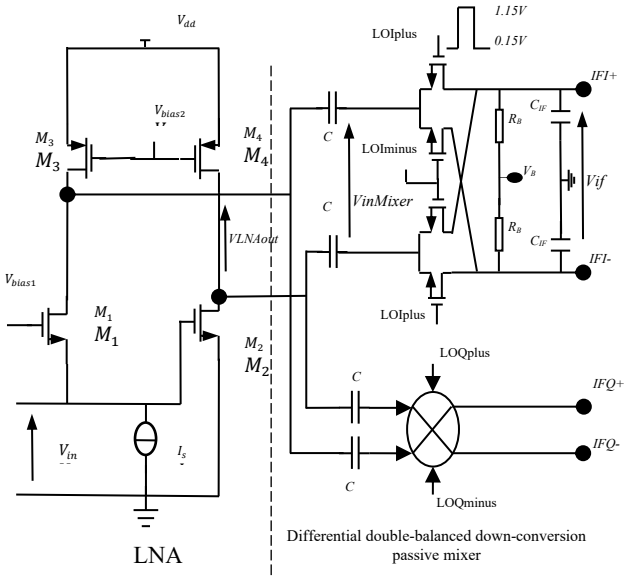

Fig. 9. Passive mixer-based UWB receiver circuit

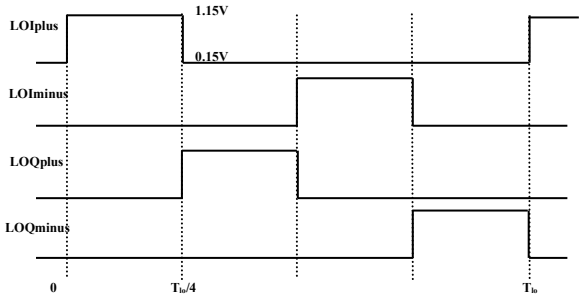

Fig. 10. Time representation of LO rectangular signals with a 25% duty cycle

As illustrated in Fig. 10, four rectangular LO signals are employed to operate the NMOS switches, each with a duty cycle of 25%. Because there are no overlap periods between the LO phases, the 25% duty cycle is unaffected by LO rise and fall times, resulting in enhanced NF and linearity. Unlike the 50% duty cycle mixer, this can interfere at any moment.

To reduce the mixer sensitivity to process, voltage and temperature (PVT) changes, complete NMOS switching must be ensured. Therefore, the voltage of the LO signal must satisfy the following inequality:

$\mathrm{LOvoltage} > V_B + V_{\mathrm{inmixer}} + V_{GS}$, where Vinmixer is the voltage variation of the RF signal at the mixer input and VGS is the voltage necessary for the conduction of the transistors.

In this design, we set V_B to 0.3V and the rectangular LO signals to have a maximum LO voltage of 1.15V.

B. *Receiver simulation results*

1) *Simulation results in time domain*

Given that the proposed receiver is a time-variant circuit, we start by presenting its time domain simulation. The LO frequency is set at 4 GHz, and the duty cycle equals to 25%. Fig. 11 shows the time representation of the Vin, VinMixer and Vif signals corresponding to one period of the baseband signal (Vif).

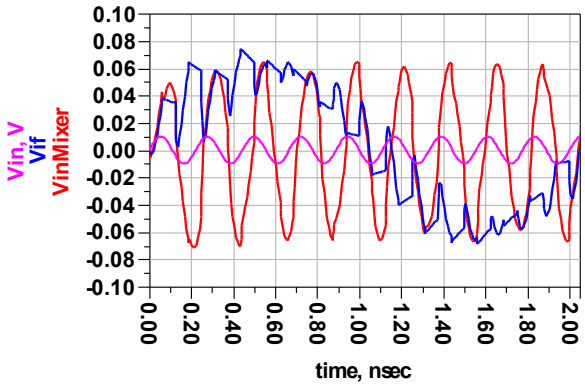

Fig. 11. Time representation of Vin, VinMixer and Vif.

Fig. 12 shows the time domain simulation results at each node of the UWB receiver circuit from the RF side to the IF side of the circuit shown in Fig. 9.

The receiver output spectrum (Vif_spectrum) and the up-converted signal spectrum (VinMixer_spectrum) are presented in Fig. 13.

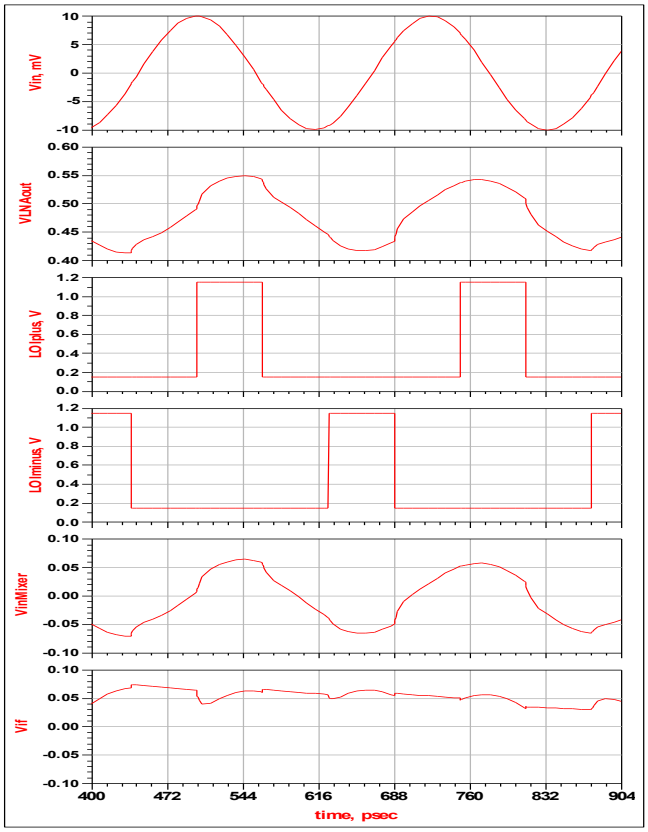

Fig. 12. Time representation of Vin, VLNAout, LOIplus, LOIminus, VinMixer and Vif signals

Fig. 12 shows the time domain simulation results at each node of the UWB receiver circuit from the RF side to the IF side of the circuit shown in Fig. 9.

The receiver output spectrum (Vif_spectrum) and the up-converted signal spectrum (VinMixer_spectrum) are presented in Fig. 13.

Vif_spectrum include the IF constituent of interest is located at (f_{RF}–f_{LO}= 0.5 GHz), the image constituent is located at (f_{RF} + f_{LO}= 8.5 GHz) and the odd high order harmonics and inter modulation products are located at ($3f_{LO} – f_{RF}$ = 7.5 GHz). This intermodulation product component is 16.7 dB under the component of interest level. Given the transparency property of this mixer, it simultaneously down-converts the RF signals (VinMixer) to IF signals (Vif) and up-converts those to RF.

The up-converted voltage spectrum (i.e. VinMixer_spectrum) contains the RF component at the mixer input (f_{RF}=4.5 GHz) and the harmonics component at (7.5 GHz + f_{LO} = 11.5 GHz) that is outside the UWB frequency range (3.1–10.6 GHz).

The RF feed through rejection (at 4.5 GHz) is 78 dB and the LO feed through rejection (at 4 GHz) is 60 dB. These results show that the proposed receiver with the down-conversion differential double-balanced passive mixer has a good ports isolation performance.

Table I indicates that the receiver exhibits an excellent conversion gain of approximately 16 dB, while the differential double-balanced passive mixer incurs a conversion loss of approximately 0.13dB only. These values are very competitive.

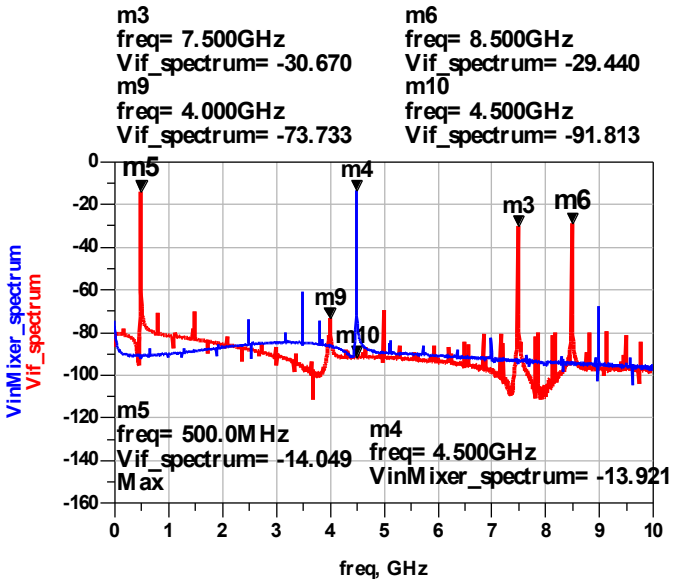

Fig. 13. Receiver output spectrum (Vif_spectrum) and mixer input spectrum (VinMixer_spectrum) in dBm

TABLE I
CONVERSION GAIN OF THE RECEIVER (RX) AND THE MIXER

Conv_GainMixer	Conv_G_dBMixer	Conv_GainRx	Conv_G_dBRx
0.985	-0.128	6.275	15.952

2) Receiver linearity performance

We run on ADS tool harmonic balance simulation to determine the linearity performance of the receiver. Fig. 14 shows the receiver gain versus the LNA input power in dBm. The receiver achieves a gain of more than 16 dB for an input power less than 20 dBm which is regarded as a good value.

Fig. 15 shows that the 1dB compression point P_{-1dB} equals to -12.77 dBm. To evaluate the distortion performance of the receiver's front end, a simulation was conducted for third and second-order inter modulation intercept inputs IIP3 and IIP2 as shown in Fig. 16 and Fig. 17. An IIP3 of 3.14 dBm and an IIP2 of 17.5 dBm were achieved.

The proposed mixer-based UWB receiver front end consumes 7.6 mW from a 1.8-V power supply, while the passive mixer consumes nearly zero power (0.72 pW).

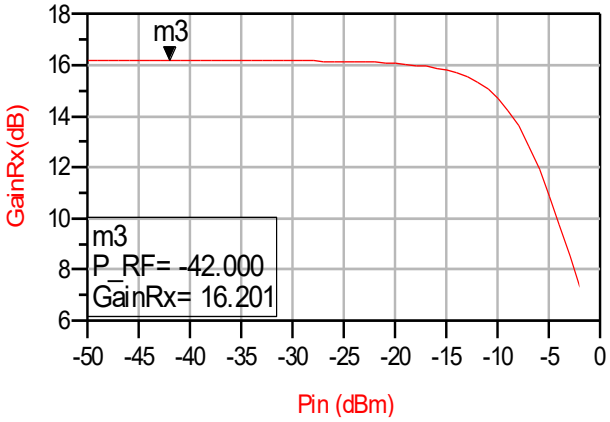

Fig. 14. Receiver gain

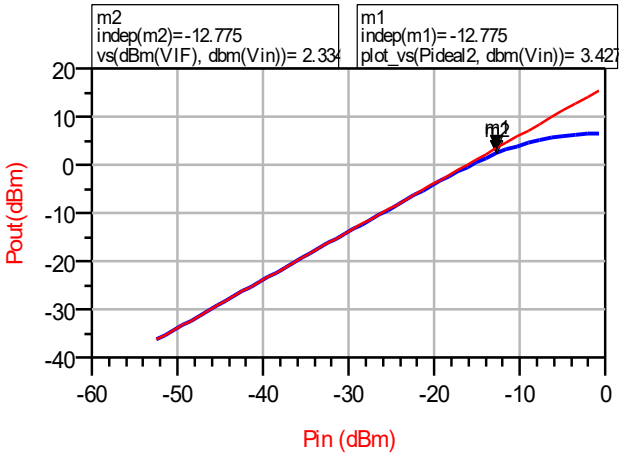

Fig. 15. P_{-1dB} of the receiver

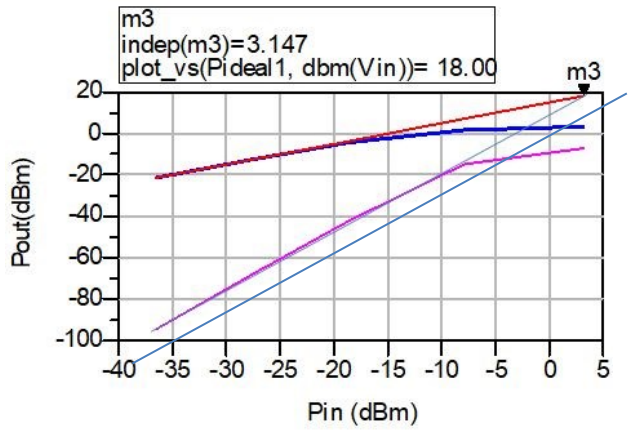

Fig. 16. IIP3 of the receiver

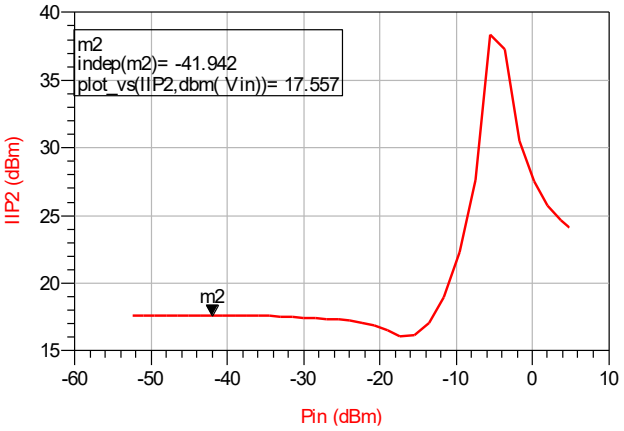

Fig. 17. IIP2 of the receiver

Table II shows a comparison with previously published UWB receivers. We can see that the proposed double balanced passive mixer-based UWB receiver archives the best performances in term of linearity, input return loss, ports isolation and power consumption. Also the proposed LNA circuit has the highest gain and a comparative noise figure to the other references.

TABLE II
COMPARISON WITH PREVIOUSLY PUBLISHED RECEIVERS

	This work	[3]	[23]	[24]	[25]	[26]
CMOS technology (nm)	180	180	180	90	180	180
Bandwidth (GHz)	3-5	3-5	3.15–3.9	3-5	3-5	3-5
LNA gain (dB)	25.3	16.8	18	15	17	15
LNA NF (dB)	2.9	2.6-3.1	10	3.1	2.5-3.5	5.2
Receiver gain (dB)	16	15	31	6	8	23.2
Receiver IIP3 (dBm)	3.14	-3.4	-15	-	0.5	1
Receiver S11 (dB)	<-12.5	<-10.1	<-9	<-10	<-12	<-9.5
Port isolation (dB) LO_IF - RF_IF	60-78	-	25-25	-	-	-
Receiver power cons. (mW)	7.6	35.1	99	22.3	26.6	18

V. CONCLUSION

In this study, a differential passive mixer-based UWB receiver front-end was designed and analyzed, using TSMC RF 0.18 µm CMOS process. The front-end circuit utilizes an inductorless balun LNA and a 25% duty cycle double-balanced passive mixer. Operating at 3–5 GHz, the receiver front-end exhibits a gain of 16 dB an IIP3 of 3.14dBm and an IIP2 with 17.5 dBm leading to improved linearity.

The designed receiver demonstrated an excellent RF and LO feed through rejection. Therefore the proposed double balanced passive mixer-based UWB receiver with differential topology is a good candidate to be integrated in a single chip UWB transceiver for WBAN medical application.

REFERENCES

[1] L. Xia, K. Shao, H. Chen, Y. Huang, Z. Hong, and P. Y. Chiang, "0.15-nJ/b 3–5-GHz IR-UWB system with spectrum tunable transmitter and merged-correlator noncoherent receiver," IEEE Trans. Microw. Theory Tech., vol. 59, no. 4, pp. 1147–1156, 2011. http://doi.org/10.1109/TMTT.2011.2114193

[2] L. Liu, T. Sakurai, and M. Takamiya, "A charge-domain auto-and cross-correlation based data synchronization scheme with power-and area-efficient PLL for impulse radio UWB receiver," IEEE J. Solid-State Circuits, vol. 46, no. 6, pp. 1349–1359, 2011. http://doi.org/10.1109/JSSC.2011.2128210

[3] Jihai Duan, Q. Hao2, Y. Zheng, B. Wei, W. Xu, and S. Xu, "Design of an Incoherent IR-UWB Receiver Front-End in 180-nm CMOS Technology." 16th IEEE International Symposium on Quality Electronic Design (ISQED), pp. 186-190, 2015. http://doi.org/10.1109/ISQED.2015.7085422

[4] B. Shi and M. Y. W. Chia, "Design of a CMOS UWB receiver front-end with noise-cancellation and current-reuse," in 2010 IEEE International Conference on Ultra-Wideband, vol. 1, pp. 1–4, 2010. http://doi.org/10.1109/ICUWB.2010.5614618

[5] H. Trabelsi, I. Barraj, and M. Masmoudi, "A 3–5 GHz FSK-UWB transmitter for wireless personal healthcare applications," AEU-International J. Electron. Commun., vol. 69, no. 1, pp. 262–273, 2015. http://doi.org/10.1016/j.aeue.2014.09.009

[6] B. Saif and T. Hatem, "Low-complexity passive mixer-based UWB pulse generator with leakage compensation and spectrum Tunability," in 2020 IEEE International Conference on Design & Test of Integrated Micro & Nano-Systems (DTS), pp. 1–5, 2020. http://doi.org/10.1109/DTS48731.2020.9196120

[7] S. Benali and H. Trabelsi, "Analysis of device mismatches effect on the performance of UWB-Ring VCO," in 2020 17th International Multi-Conference on Systems, Signals & Devices (SSD), pp. 814–818, 2020. http://doi.org/10.1109/SSD49366.2020.9364258

[8] R. S. Rao, Microwave engineering. PHI Learning Pvt. Ltd., 2015.
[9] B. Razavi and R. Behzad, RF microelectronics, vol. 2. Prentice hall New York, 2012.
[10] B. Razavi et al., "A 0.13/spl mu/m CMOS UWB transceiver," in ISSCC. 2005 IEEE International Digest of Technical Papers. Solid-State Circuits Conference, pp. 216–594, 2005. \http://doi.org/10.1109/ISSCC.2005.1493946
[11] C. Sandner et al., "A wimedia/mboa-compliant cmos rf transceiver for uwb," IEEE J. Solid-State Circuits, vol. 41, no. 12, pp. 2787–2794, 2006. http://doi.org/10.1109/JSSC.2006.884804
[12] Y. Zheng et al., "A CMOS carrier-less UWB transceiver for WPAN applications," in 2006 IEEE International Solid State Circuits Conference-Digest of Technical Papers, pp. 378–387, 2006. http://doi.org/10.1109/ISSCC.2006.1696069
[13] E. C. M. Association, "High rate ultra wideband PHY and MAC standard," Stand. ECMA-368 2nd Ed., 2007.
[14] M. Y. Algumaei, N. A. Shairi, Z. Zakaria, and I. M. Ibrahim, "Review of mixer and balun designs for UWB applications," Int. J. Appl. Eng. Res., vol. 12, no. 17, pp. 6514–6522, 2017.
[15] F. Marki and C. Marki, "Mixer basics primer," Marki Microw., 2010.
[16] H. Khosravi, A. Bijari, N. Kandalaft and J. Cabral, "A Low Power Concurrent Dual-Band Low Noise Amplifier For WLAN Applications," *2019 IEEE 10th Annual Information Technology, Electronics and Mobile Communication Conference (IEMCON)*, pp. 1118-1123, 2019. http://doi.org/10.1109/IEMCON.2019.8936211
[17] R. Bagheri et al., "An 800-MHz–6-GHz software-defined wireless receiver in 90-nm CMOS," IEEE J. Solid-State Circuits, vol. 41, no. 12, pp. 2860–2876, 2006. http://doi.org/10.1109/JSSC.2006.884835
[18] F. Bruccoleri, E. A. M. Klumperink, and B. Nauta, "Wide-band CMOS low-noise amplifier exploiting thermal noise canceling," IEEE J. Solid-State Circuits, vol. 39, no. 2, pp. 275–282, 2004. http://doi.org/10.1109/JSSC.2003.821786
[19] S. C. Blaakmeer, E. A. M. Klumperink, D. M. W. Leenaerts, and B. Nauta, "Wideband balun-LNA with simultaneous output balancing, noise-canceling and distortion-canceling," IEEE J. Solid-State Circuits, vol. 43, no. 6, pp. 1341–1350, 2008. http://doi.org/10.1109/JSSC.2008.922736
[20] C.-F. Liao and S.-I. Liu, "A broadband noise-canceling CMOS LNA for 3.1–10.6-GHz UWB receivers," IEEE J. Solid-State Circuits, vol. 42, no. 2, pp. 329–339, 2007. http://doi.org/10.1109/CICC.2005.1568632
[21] B. Mouna, B. Saif, B. Ghazi, and T. Hatem, "Analysis and Optimization of RF Front-End for MICS Band Receiver," in 2019 IEEE International Conference on Design & Test of Integrated Micro & Nano-Systems (DTS), pp. 1–5, 2019. http://doi.org/10.1109/DTSS.2019.8914911
[22] W. Xie, X. Li, and X. Long, "Underground Operator Monitoring Platform Based on Ultra-Wide Band WSN.," Int. J. Online Eng., vol. 14, no. 10, 2018.
[23] M. U. Nair, Y. Zheng, C. W. Ang, Y. Lian, X. Yuan and C. -H. Heng, "A Low SIR Impulse-UWB Transceiver Utilizing Chirp FSK in 0.18 µm CMOS," in IEEE Journal of Solid-State Circuits, vol. 45, no. 11, pp. 2388-2403, Nov. 2010, http://doi.org/10.1109/JSSC.2010.2074232
[24] Z. Zou et al., "A low-power and flexible energy detection IR-UWB receiver for RFID and wireless sensor networks," IEEE Trans. Circuits Syst. I Regul. Pap., vol. 58, no. 7, pp. 1470–1482, 2011. http://doi.org/10.1109/TCSI.2011.2142930
[25] T. A. Vu, H. A. Hjortland, O. Nass, and T. S. Lande, "A 3-5 GHz IR-UWB receiver front-end for wireless sensor networks," Proceedings - IEEE International Symposium on Circuits and Systems. pp. 2380–2383, 2013, http://doi.org/10.1109/ISCAS.2013.6572357
[26] G. Cusmai, M. Brandolini, P. Rossi and F. Svelto, "A 0.18-µm CMOS Selective Receiver Front-End for UWB Applications," in IEEE Journal of Solid-State Circuits, vol. 41, no. 8, pp. 1764-1771, Aug. 2006, http://doi.org/10.1109/JSSC.2006.877256.